bioRxiv preprint doi: https://doi.org/10.1101/067173; this version posted August 1, 2016. The copyright holder for this preprint (which was not certified by peer review) is the author/funder, who has granted bioRxiv a license to display the preprint in perpetuity. It is made available under aCC-BY-NC-ND 4.0 International license.

# Stochastic Assembly Produces Heterogeneous Communities in the *C. elegans* Intestine

[1]Nicole M. Vega and [1]Jeff Gore

[1]Physics of Livings Systems, Department of Physics, Massachusetts Institute of Technology, Cambridge, MA, 02139, USA

Correspondence: nvega@mit.edu or gore@mit.edu

bioRxiv preprint doi: https://doi.org/10.1101/067173; this version posted August 1, 2016. The copyright holder for this preprint (which was not certified by peer review) is the author/funder, who has granted bioRxiv a license to display the preprint in perpetuity. It is made available under aCC-BY-NC-ND 4.0 International license.

**Abstract**

Host-associated bacterial communities vary extensively between individuals, but it can be very difficult to determine the sources of this heterogeneity. Here we demonstrate that stochastic bacterial community assembly in the *C. elegans* intestine is sufficient to produce strong inter-worm heterogeneity in community composition. When worms are fed with two neutrally-competing fluorescently labeled bacterial strains, we observe stochastically-driven bimodality in community composition, where approximately half of the worms are dominated by each bacterial strain. A simple model incorporating stochastic colonization suggests that heterogeneity between worms is driven by the low rate at which bacteria successfully establish new intestinal colonies. We can increase this rate experimentally by feeding worms at high bacterial density; in these conditions the bimodality disappears. These results demonstrate the potential importance of stochastic processes in bacterial community formation and suggest a role for *C. elegans* as a model system for ecology of host-associated communities.

**Introduction**

The gut microbiome varies greatly between individuals, and this variation could have important health consequences (1,2). These differences may be due to genetic differences between individuals, to differences in individual history and environmental exposure, and to stochasticity (3,4), but the relative contributions of these factors are difficult to determine. Extensive research has focused on the deterministic factors directing microbial community composition (5–7). Indeed, the canonical understanding of community assembly is based on deterministic niche-based processes, which push communities toward equilibria determined by the species present and the resources available. Under this view, if individual hosts are exposed to similar species and contain similar environmental conditions, they are expected to converge to similar community compositions. By contrast, where stochastic processes dominate, similar hosts exposed to identical environmental conditions can diverge considerably in their final community composition. This will be the case where migratory and other

bioRxiv preprint doi: https://doi.org/10.1101/067173; this version posted August 1, 2016. The copyright holder for this preprint (which was not certified by peer review) is the author/funder, who has granted bioRxiv a license to display the preprint in perpetuity. It is made available under aCC-BY-NC-ND 4.0 International license.

random processes outweigh any deterministic differences between colonizing species, such as competitive ability. While the stochastic processes of migration and drift are known to be important in determining the composition of natural communities (8,9), it is generally difficult to experimentally quantify the the effects of stochasticity on community formation.

This is of particular interest in host-associated microbial communities, where a great deal of variation can be observed between individuals, and the role of stochastic processes in producing and maintaining this heterogeneity is not well understood. Despite substantial evidence for a core intestinal microbiota in multiple organisms (1,10–12), an increasing body of evidence suggests that stochastic processes may be generally important in determining the structure of host-associated communities (13–15).

*C. elegans* is used in these experiments as a tractable experimental model of a gastrointestinal system undergoing bacterial colonization (16). The nematode has been used extensively as a laboratory organism and has many desirable properties, including selfing hermaphroditism (allowing maintenance of homozygous cultures), transparency under light microscopy, ease of culture, a short life cycle, and rapid generation time. Using the worm, it is therefore possible to generate large numbers of nearly genetically identical individuals with identical life histories, which can be colonized under identical conditions to allow observation of the stochastic forces underlying microbial community assembly.

**Results**

To explore the role of stochastic colonization of an intestinal environment, we colonized *C. elegans* by allowing synchronized adult worms to feed for eight days on a 50/50 mixture of live *E. coli* fluorescently labeled with YFP or dsRed (**Fig. 1A**). Worms were colonized in liquid culture to ensure that all worms experienced a uniform environment without opportunities for selective feeding. Most worm intestines were successfully colonized by the bacteria, with an average of ~35,000 ± 7,000 colony forming units (CFU) per worm (N = 53 colonized/56 total worms, mean ± s.e.m.). As expected, dilution plating of disrupted worm communities confirmed that the average community composition across all worms was close to 50/50 for the two colors (average 58% dsRed,

bioRxiv preprint doi: https://doi.org/10.1101/067173; this version posted August 1, 2016. The copyright holder for this preprint (which was not certified by peer review) is the author/funder, who has granted bioRxiv a license to display the preprint in perpetuity. It is made available under aCC-BY-NC-ND 4.0 International license.

**Fig. 1B**).

Given the large population sizes within the worm intestines and the fact that the worms were fed well-mixed bacteria at equal ratios, it would be natural to assume that the individual intestinal communities would also show a 50/50 mixture of the two colors of bacteria. However, though the average across all worms was close to the expected ratio, dilution plating of the intestinal communities of individual worms revealed that each worm tended to be dominated by one of the two colors, resulting in a bimodal distribution of community compositions (**Fig. 1B,C**). The intestinal communities within individual worms therefore display a striking difference from the 50/50 mixture present within the bacterial population present outside of the worm.

In the absence of deterministic factors such as competitive differences or life history differences between hosts, we conclude that the striking variation between individuals results from stochasticity in the initial colonization of the intestine. Indeed, fluorescent images of the colonized worms (**Fig 1C**) revealed a patchy distribution of the two bacteria strains in the intestine, consistent with rare colonization events leading to distinct colonies. To further explore this hypothesis, we measured consumption rates and found that ~50 bacteria were consumed per worm per hour at the bacterial density used in feeding (**Fig. 2A)**, meaning that each worm consumed ~$10^4$ live bacteria over the course of the experiment; bimodality was observed despite the large number of potential colonists, consistent with prior observations that a small fraction of ingested bacteria survive to colonize the *C. elegans* intestine (17). Indeed, we found that less than 1 in 1000 of the bacteria consumed by the worm both survive the feeding and successfully adhere to the intestine (**Fig. 2A**), thus providing a potential explanation for the source of stochasticity that leads to bimodality in community composition.

To gain insight into the process of stochastic colonization and growth, we constructed a minimal model which incorporates stochastic colonization of the worm at rate *c,* birth rate *b,* saturated population size *K*, and death rate *d* which includes both death and excretion out of the worm (**Table 1**, **Fig. 3A, Fig. S1**). The generalized system of reactions for these simulations is:

bioRxiv preprint doi: https://doi.org/10.1101/067173; this version posted August 1, 2016. The copyright holder for this preprint (which was not certified by peer review) is the author/funder, who has granted bioRxiv a license to display the preprint in perpetuity. It is made available under aCC-BY-NC-ND 4.0 International license.

$$\emptyset \xrightarrow{(bN_i+c)\left(1-\frac{\sum N}{K}\right)} N_i$$

$$N_i \xrightarrow{dN_i} \emptyset$$

where $i$={1,2} denotes the index of the neutrally-competing bacterial strain. Strains are identical apart from their index and use the same values for *b, d, K,* and *c*. Stochastic simulations were implemented using the Gillespie algorithm (18) (**Fig. 3A**). Notably, for a simplified version of the birth-death-immigration process where we ignore saturation, the full time-dependent solution can be found analytically (19).

Colonization rate in this context corresponds to the rate at which bacteria survive being consumed and successfully adhere to the gut. We determined that growth of bacteria in the *C. elegans* intestine in the absence of colonization is highly variable, but average population size over time can be described by a logistic model (**Fig. 2A**), consistent with previous reports in zebrafish (20) In this system, colonization rate (number of live intestinal bacteria obtained from the environment per unit time) is an experimentally tunable parameter which depends on the density of bacteria outside the worms (**Fig. 2A**).

In our stochastic model, we expect that the variation between communities in individual worms will depend on the relative magnitude of two time-scales: (1) the typical time between successive successful colony establishment events ($T_{est}=\frac{1}{c\left(1-p_{ext}\right)}=\frac{b}{c\left(b-d\right)}$, where $p_{ext}=d/b$ is the probability of a new colonist going extinct (21)) and (2) the timescale associated with net exponential growth of a colony once established ($T_{grow}=1/\left(b-d\right)$) (**Fig. 3B,C**). As can be seen from these equations, the establishment time $T_{est}$ is determined by the rate of colonization and the birth and death rates, since these together influence the probability that an initial migrant will successfully start a new colony within the worm. If $T_{est} \ll T_{grow}$, new colonists are expected to arrive rapidly relative to the time it takes a colony to grow; the distribution of bacteria within each intestine will be forced by the external bacterial population, resulting in worm-associated colonies that are very similar to both the pool of colonists and to one another. However, if $T_{est} \gg T_{grow}$,, successful colonists are expected to be rare and a given colonist is expected to have a long time to grow and fill the host gut before another successful colonist

bioRxiv preprint doi: https://doi.org/10.1101/067173; this version posted August 1, 2016. The copyright holder for this preprint (which was not certified by peer review) is the author/funder, who has granted bioRxiv a license to display the preprint in perpetuity. It is made available under aCC-BY-NC-ND 4.0 International license.

arrives, resulting in worms that are dominated by the single-color offspring of their first successful colonist.

Which regime we are in therefore depends upon the ratio $\frac{T_{grow}}{T_{est}} = \frac{c}{b}$. Biologically, birth rate *b* is fixed within a fairly narrow range of values (less than a full order of magnitude), capped by the maximum physiological growth rate of the bacteria and bounded below by the death rate in this system. However, the colonization rate *c* can be easily tuned over several orders of magnitude by changing the density of bacteria on which the worms are allowed to feed **(Fig. 2)**. The model thus predicts that if we increase the colonization rate *c* then the bimodality will disappear, and each intestinal community will approach a 50/50 mixture of the two labeled bacteria.

To test this hypothesis, we fed worms at a range of higher bacterial cell densities, thus increasing the colonization rate (**Fig 4A**). As expected from the model, as bacterial concentrations outside the worm increase, the resulting intestinal communities become more similar to one another (**Fig. 4A**), and the distribution of populations goes from bimodal to unimodal (**Fig. 4B**). Specifically, at high bacterial density, each worm has a microbial community that is reflective of the 50/50 mixture of red/green bacteria present outside of the worm. The strength of stochastic forces in determining the composition of the worm intestine therefore depends strongly on the feeding rate of the worm. Despite the fact that these bacteria compete neutrally in the absence of worms (**Fig. S2**) and colonize worms at comparable rates (**Fig. S3**), populations inside the worms show a slight excess of dsRed-labeled bacteria for reasons that are not clear (**Fig 4B**).

A prediction of our model (**Fig. 3**) is that the transition from bimodality to unimodality does not depend upon the carrying capacity of the worm, since the bimodality arises from initial differences in colonization time that are "frozen in" to the final distribution without regard to final population size. To test this prediction, we take advantage of the fact that the population size of the gut community depends strongly on the functioning of the immune system of the worm. The experiments described so far were performed in an immune-compromised worm strain capable of supporting large bacterial populations (AU37), whereas the wild-type worm strain (N2) with normal immune function has a bacterial population size that is an order of magnitude lower (~4400 bacteria per worm as compared to the 35,000 observed previously). Consistent with predictions from the model, the

bioRxiv preprint doi: https://doi.org/10.1101/067173; this version posted August 1, 2016. The copyright holder for this preprint (which was not certified by peer review) is the author/funder, who has granted bioRxiv a license to display the preprint in perpetuity. It is made available under aCC-BY-NC-ND 4.0 International license.

transition from bimodality to unimodality also occurs in the wild-type worm, and this transition occurs at a similar density of bacteria (**Fig. S4**). Our experimental observation of heterogeneity in gut populations driven by stochastic colonization is therefore was robust to host genotype, even when the different hosts result in steady-state bacterial population sizes that are different by more than an order of magnitude.

To determine whether stochastic colonization also plays a role in inter-species competition within the gut, we fed *C. elegans* on a 50/50 mixture of *Enterobacter aerogenes* and *Serratia marcescens*, both Gram-negative bacteria from the family *Enterobacteriaceae*. Unlike the single species case, the resulting communities were not distributed around the 50/50 mark but had a median of 10-20% *E. aerogenes*, indicating a probable selective advantage for *S. marcescens* in the worm intestine. Under conditions where colonization is rapid (worms fed at ~$10^8$ CFU/mL), the distribution of populations in individual worms had a visible central tendency at 10-20% *E. aerogenes*, consistent with the median behavior of the set of populations as a whole (**Fig. 4C**). Under slow colonization conditions (worms fed at ~$10^6$ CFU/mL), however, the worm intestinal communities tend to be entirely dominated by one of the two species (**Fig. 4C**). It should be noted that even at high migration rates there is still a minority of worms that are dominated by the *E. aerogenes* despite the fact the distribution is peaked at 10 – 20% *E. aerogenes*, highlighting that interspecies competition will likely result in richer dynamics than are present with neutral labels. Nonetheless, these data suggest that the effects of stochastic colonization may be relevant in determining the composition of diverse communities.

**Discussion**

Though the bimodality that we observe in community composition with neutral labels can be explained by a simple stochastic model, the real data show more variation than predicted by the model. In particular, there is more variation in the number of bacteria per worm than can be explained using our simple model (**Fig. S5**). Further, the transition from bimodality to unimodality occurs at a bacterial feeding density of ~$10^8$ CFU/mL rather than the $10^7$ CFU/mL that would be predicted by the model using our estimates of parameters such as the net colonization rate (**Fig. 3C, 4B**), although this divergence could be explained by the uncertainty around our point estimates for these parameters. This suggests that the simple model used here does not account for one or

bioRxiv preprint doi: https://doi.org/10.1101/067173; this version posted August 1, 2016. The copyright holder for this preprint (which was not certified by peer review) is the author/funder, who has granted bioRxiv a license to display the preprint in perpetuity. It is made available under aCC-BY-NC-ND 4.0 International license.

more important sources of variance. For example, despite the use of age-synchronized adult worms, there may be variation between host environments; that is, the demographic parameters directing community formation may vary among individual hosts. Indeed, considerable heterogeneity in "effective age" of individuals has been observed within synchronized cultures of *C. elegans*, resulting in heterogeneity in stress resistance and lifespan (22,23). In addition, the demographics of bacterial growth and death may change as worms age (17,24,25), and excretion may occur in "pulses" rather than continuously as recently observed in a zebrafish model (26). These sources of variation could have profound effects on community composition, particularly in more complex cases where there are higher numbers of colonizing species and where the colonists do not compete neutrally, or where interactions between bacteria and host occur over evolutionary time (27).

The bimodal-to-unimodal transition with increasing colonization rate observed here resembles the expected behavior of a population behaving according to Hubbell's neutral model of island biogeography (28). Unlike our model which begins with an uncolonized "island", the Hubbell neutral model begins with an island of size $N$ which is filled to capacity, in which individuals cannot be displaced but dead individuals can be replaced through either migration from a metacommunity or reproduction from within the island. In this zero-sum model, what determines whether the population distribution is unimodal or bimodal depends not on $T_{grow}$ but rather on the typical timescale over which drift leads to extinction of a neutral lineage (which is much longer than $T_{grow}$ and scales as the square of the population size $N$).

The work presented here suggests potential for *C. elegans* as a model organism for host-associated microbiotal community formation. The worm is used here as a tractable experimental model of a gastrointestinal system undergoing bacterial colonization (16). The nematode has been used extensively as a laboratory organism and has many desirable properties, including selfing hermaphroditism (allowing maintenance of homozygous cultures), transparency under light microscopy, ease of culture, a short life cycle, and rapid generation time. Using the worm, it is therefore possible to generate large numbers of nearly genetically identical individuals with identical life histories, which can be colonized under identical conditions to allow observation of the stochastic forces underlying microbial community assembly. Previous work has shown that the worm can be colonized

bioRxiv preprint doi: https://doi.org/10.1101/067173; this version posted August 1, 2016. The copyright holder for this preprint (which was not certified by peer review) is the author/funder, who has granted bioRxiv a license to display the preprint in perpetuity. It is made available under aCC-BY-NC-ND 4.0 International license.

with a wide variety of bacterial species, including important human pathogens (29–31). *C. elegans* is a selective environment, allowing some bacterial species to thrive while preventing the growth of others, and there is some evidence for a "core" gastrointestinal microbiota in the worm (32). In addition, our model for colonization of the worm intestine invites comparisons to models of island communities (28). *C. elegans* provides a well-controlled, highly replicable environment for microbiotal experiments, and the work shown here demonstrates potential utility for future studies of stochastic and deterministic processes in community assembly.

The results presented here suggest that stochastic processes may have strong effects on host-associated microbial community assembly. Stochasticity has long been understood as a potential source of variation in these communities, but much work in this area focuses on deterministic factors such as differences between individual hosts. However, stochasticity is known to be a very important source of variation in some cases; for example, clonal heterogeneity between hosts has been observed in infectious disease, where an individual host may be dominated by a small number of strains or even a single clonal lineage, and stochastic bottlenecking during the life cycle of the disease has been implicated as a cause of this heterogeneity (33–35). Due to the effects of bottlenecking, stochastic assembly may therefore be an important factor in evolution within host-associated bacterial communities and in co-evolution of bacteria and host (36). We suggest that stochasticity as a driver of heterogeneity between individuals may be broadly important and deserving of further consideration in studies of host-associated microbiota.

## Materials and Methods

### Nematode culture

Unless otherwise stated, nematodes were cultivated under standard conditions (37), and the temperature-sensitive sterile *C. elegans* strain AU37 (*glp-4(bn2)* I; *sek-1(km4)* X) (38) was used for experiments. Due to the *glp-4* mutation, this strain is able to reproduce at 15ºC but does not develop gonads and is therefore sterile when raised at room temperature (23-25ºC); use of this strain prevented the worms from producing progeny during

bioRxiv preprint doi: https://doi.org/10.1101/067173; this version posted August 1, 2016. The copyright holder for this preprint (which was not certified by peer review) is the author/funder, who has granted bioRxiv a license to display the preprint in perpetuity. It is made available under aCC-BY-NC-ND 4.0 International license.

experiments, ensuring that all worms in a given experiment were of the same age and had the same life history. Additionally, the loss of the large hermaphrodite ovary was advantageous for microscopy due to the simplified internal tube-within-a-tube body structure. The *sek-1* mutation decreases immune function, making these worms more susceptible to bacterial colonization and allowing large intestinal bacterial communities to be readily established (38). Worm strains were provided by the Caenorhabditis Genetic Center, which is funded by NIH Office of Research Infrastructure Programs (P40 OD010440).

Synchronized cultures were obtained using standard protocols (37). For propagation of worm cultures, AU37 cultures were maintained at the permissive temperature (15°C) on NGM agar plates with lawns of the standard food organism *E. coli* OP50. N2 worms were maintained at 23ºC on NGM plates with OP50. For synchronization, we washed 4-6 nearly starved plates with sterile distilled water and treated the harvested worms with a bleach-sodium hydroxide solution; the isolated eggs were placed in M9 worm buffer overnight to hatch, then transferred to NGM + OP50 plates at the non-permissive temperature (25°C) for 3 days to obtain gonadless (sterile) synchronized adults. Adults were washed from plates using M9 worm buffer + 0.1% Triton X-100, then rinsed with M9 worm buffer and surface bleached for 10 minutes at 4°C in a 1:1000 bleach solution in M9 to remove any live OP50. Worms were then transferred to S medium + 100 µg/mL gentamycin + 5X heat-killed OP50 for 24 hours to kill any OP50 inhabiting the intestine, resulting in germ-free synchronized worms. These worms (2-3 day synchronized adults) were then rinsed in M9 worm buffer + 0.1% Triton X-100, washed via sucrose flotation to remove debris, and rinsed 3X in M9 worm buffer to remove sucrose before use in experiments.

**Bacteria**

These experiments used *E. coli* MC4100 ($F^-$ $[araD139]_{B/r}$ Δ(argF-lac)169* &lambda$^-$ e14- flhD5301 Δ(fruK-yeiR)725 (fruA25)‡ relA1 rpsL150(strR) rbsR22 Δ(fimB-fimE)632(::IS*1*) *deoC1*) carrying plasmids E3350 (pUC18T-mini-Tn7-Gm-eyfp, accession DQ493879) or E3322 ( pUC18T-mini-Tn7-Gm-DsRedExpress, accession DQ493880)(39). *E. coli* MC4100 was obtained from the *E. coli* Genetic Stock Center (CGSC #6152).

bioRxiv preprint doi: https://doi.org/10.1101/067173; this version posted August 1, 2016. The copyright holder for this preprint (which was not certified by peer review) is the author/funder, who has granted bioRxiv a license to display the preprint in perpetuity. It is made available under aCC-BY-NC-ND 4.0 International license.

For multispecies colonization experiments, *Enterobacter aerogenes* (ATCC 13048) and *Serratia marcescens* (ATCC 13880) were obtained from ATCC.

Bacterial strains were grown in individual cultures in LB + 30 µg/mL gentamycin for selection where necessary. For feeding assays, *E. coli* were grown overnight at 37ºC, and *E. aerogenes* and *S. marcescens* were grown overnight at 30ºC. Bacterial cultures were acclimated briefly (~1 hour) to room temperature before feeding. To construct feeding cultures, *E. coli* were centrifuged 1 minute at 9K RPM to pellet, washed once in S medium, then resuspended in S medium + 30 µg/mL gentamycin. As *S. marcescens* is very difficult to pellet through centrifugation, *E. aerogenes* and *S. marcescens* were diluted to ~$10^9$ CFU/mL in S medium without washing.

**Colonization of *C. elegans***

Sterile, washed adult worms were resuspended in S medium (with 30 µg/mL gentamycin for selection where needed) and moved in 900 µL aliquots to individual wells of a 24-well culture plate, with a final concentration of ~1000 worms/mL. 100 µL of bacterial suspension at 10X desired concentration was added to each well before plates were covered with a Breathe-Easy® adhesive gas-permeable membrane (USA Scientific). Plates were incubated with shaking at 300 RPM at 25ºC. For multi-day assays, worms were re-fed every 24 hours; to do this, worms were removed from wells, washed 1X with M9 worm buffer + 0.1% Triton X-100 and 2X with M9 worm buffer to remove most external bacteria, and resuspended in 900 µL fresh S medium for re-plating as previously described.

**Disruption of worms and plating of intestinal populations**

Colonized worms were washed 1X with M9 worm buffer + 0.1% Triton X-100 and 2X with M9 worm buffer to remove most external bacteria, then resuspended in 100 µL S medium + 1X heat-killed OP50 and incubated at room temperature (23ºC) for 30-60 minutes to allow the worm to purge any non-adhered bacterial cells from the intestine. Worms were then rinsed 2X with M9 worm buffer + 0.1% Triton X-100, chilled briefly to stop peristalsis, and surface bleached for 10 minutes at 4C in 100 µL M9 worm buffer with commercial bleach at 1:1000 concentration.

bioRxiv preprint doi: https://doi.org/10.1101/067173; this version posted August 1, 2016. The copyright holder for this preprint (which was not certified by peer review) is the author/funder, who has granted bioRxiv a license to display the preprint in perpetuity. It is made available under aCC-BY-NC-ND 4.0 International license.

For manual disruption, bleached worms were rinsed 1X in M9 worm buffer + 0.1% Triton X-100 to remove bleach, then transferred to 3 mL M9 worm buffer + 1% Triton X-100 in a small (40 cm) petri dish (Fisher Scientific). Individual worms were pipetted out in 20 µL aliquots of buffer and transferred to 0.5 mL clear microtubes (Kimble Kontes) for manual disruption with a motorized pestle (Kimble Kontes Pellet Pestle with blue disposable pestle tips, Fisher Scientific). Magnification was provided by a magnifying visor (Magni-Focuser Hands Free Binocular Magnifier 3.5X). After disruption, tubes were centrifuged 2 minutes at 12K RPM to collect all material, and the resulting pellet was resuspended in 180 µL M9 worm buffer (final volume 200 µL/worm) before transfer to 96-well plates for serial dilution in 1X phospho-buffered saline (PBS).

For 96-well plate disruption, bleached worms were rinsed 1X in M9 worm buffer + 0.1% Triton X-100 to remove bleach. Worms were then treated for 20 minutes with 100 µL of a SDS/DTT solution in M9 worm buffer (0.25% sodium dodecyl sulfate + 3% freshly mixed dithiothrietol, chemicals from Sigma Aldrich), rinsed with 150 µL M9 worm buffer, then rinsed again in 1 mL M9 worm buffer + 0.1% Triton X-100 before transfer to 3 mL M9 worm buffer + 1% Triton X-100 in a small (40 cm) petri dish (Fisher Scientific). A deep-well plate (2 mL square well plate, Axygen) was prepared by addition of a small quantity of sterile autoclaved 36-mesh silicon carbide grit (Kramer Industries) to each well, followed by addition of 180 µL M9 worm buffer + 1% Triton X-100. Individual worms were then pipetted out in 20 µL aliquots of buffer and transferred to individual wells of the plate. The plate was covered with parafilm and allowed to chill for at least one hour prior to disruption to reduce heat damage to bacteria. Parafilmed plates were capped with 96-well square silicon sealing mats (Axygen Impermamat AxyMat Sealing Mats) and disrupted by shaking in a 96-well plate shaker (MO-BIO Laboratories, shaking at 30 hz for 1.5 minutes before flipping plate and shaking an additional 1.5 minutes to ensure even disruption). Plates were then centrifuged at 2500 x g for 2 minutes to collect all material in the bottom of the wells, then all plate contents were resuspended by pipetting and transferred to 96-well plates for serial dilution in PBS.

**Bimodality**

Bimodality was assessed using the bimodality coefficient (40):

bioRxiv preprint doi: https://doi.org/10.1101/067173; this version posted August 1, 2016. The copyright holder for this preprint (which was not certified by peer review) is the author/funder, who has granted bioRxiv a license to display the preprint in perpetuity. It is made available under aCC-BY-NC-ND 4.0 International license.

$$BC = \frac{m_3^2 + 1}{m_4 + 3\frac{(n-1)^2}{(n-2)(n-3)}}, m_3 \equiv skewness, m_4 \equiv excesskurtosis$$

with the canonical value of $BC_{crit} = 0.55$ used to mark the transition from a unimodal to a bimodal distribution. Calculations were implemented in Python using scipy.stats.

**Parameter estimation**

*Growth rate and carrying capacity.* Birth rate *b* and carrying capacity *K* were estimated simultaneously by fitting a logistic growth model to data for growth of bacteria inside the worm (**Fig. 2**). Briefly, *C. elegans* AU37 was fed on live *E. coli* MC4100 at ~$10^9$ CFU/mL for two days, then washed 1X with M9 worm buffer + 0.1% Triton X-100 and 2X with M9 worm buffer to remove most external bacteria, then resuspended in 1 mL S medium + 2X heat-killed OP50 in a 24-well plate, covered with a BreatheEasy membrane, and incubated at 25ºC for 10 days. To minimize new colonization, worms were washed and re-fed in fresh S medium + 2X heat-killed *E. coli* OP50 at 24-hour intervals, and 12 worms were surface bleached and individually digested for CFU plating.

Maximum growth rate was estimated by allowing *E. coli* MC4100 bacteria to grow outside the worm in S medium + 2X heat-killed OP50 at 25ºC - essentially identical to culture conditions used in worm assays, but without the worm environment. Due to the high turbidity of the medium with heat-killed OP50, CFU counts over time were determined via dilution plating.

*Net growth rate.* From the data in **Figure 2**, we observed that the net growth rate of *E. coli* MC4100 inside the worm intestine was very low, ~0.06 $hr^{-1}$. In this context, net growth rate is (births-deaths). This low net growth rate implies that birth and death rates inside the worm are very close to one another. The existence of zero counts (empty worms) in the first days of outgrowth implies that stochastic extinction in lightly-colonized worms occurs at an observable frequency, consistent with expectations for small populations where birth is only slightly more likely than death. (We must also note that the lack of uncolonized worms at later time points implies that some colonization is occurring during the outgrowth period, due to growth of excreted bacteria in the liquid

bioRxiv preprint doi: https://doi.org/10.1101/067173; this version posted August 1, 2016. The copyright holder for this preprint (which was not certified by peer review) is the author/funder, who has granted bioRxiv a license to display the preprint in perpetuity. It is made available under aCC-BY-NC-ND 4.0 International license.

environment in the 24 hours between washes.

As it is very difficult to estimate birth rate inside the worm in isolation, we are forced to extrapolate. The net growth rate (*b*-*d*) should be small, and as stated in the main text, there is a large amount of variation in bacterial population size between worms; in the context of a stochastic simulation, we therefore choose values of *b* and *d* which are as large as possible given the physiological constraints of the system in order to maximize stochastic noise. For simulations, we use the estimated growth rate of *E. coli* MC4100 outside the worms in these growth conditions (~0.6 $hr^{-1}$) as a maximum birth rate and choose a death rate of 0.54 $hr^{-1}$ to produce a net growth rate of 0.06 $hr^{-1}$.

*Excretion and death rates.* Total death and excretion were estimated using a chloramphenicol exposure assay, where chloramphenicol at concentrations above the MIC for this bacterial strain are used to prevent bacterial division without causing cell death. Here, change in CFU/worm over time is used to estimate total death, and change in CFU/mL outside the worms is used to estimate excretion (which in our model is incorporated into the cell death term *d*).

Briefly, worms were colonized with *E. coli* MC4100 E3350 or E3322 at ~$10^9$ CFU/mL for 2 days, then rinsed and purged of non-attached bacteria as previously described. Worms were then washed 1X in M9 worm buffer + 0.1% Triton X-100, surface bleached as previously described, and moved to 1 mL S medium + 0.2X heat-killed OP50 + chloramphenicol at a range of concentrations (0, 10, 20, 50, 100, and 200µg/mL) in a 24 well plate covered with BreatheEasy membrane. The plate was incubated with shaking at 300 RPM at 25ºC for 48 hours; samples of supernatant and batch worm digests (160-230 worms/digest) were taken for all conditions at 0, 24, and 48 hours.

Excretion was estimated from CFU/mL counts outside the worms at 24 hours over this range of chloramphenicol concentrations (**Fig S1A**). From these data, excretion rates are approximately 1 CFU/$10^3$-$10^4$ intestinal CFU/hr. Excretion therefore appears to account for only a small fraction of total cell death in intestinal bacteria in the worm.

bioRxiv preprint doi: https://doi.org/10.1101/067173; this version posted August 1, 2016. The copyright holder for this preprint (which was not certified by peer review) is the author/funder, who has granted bioRxiv a license to display the preprint in perpetuity. It is made available under aCC-BY-NC-ND 4.0 International license.

Death rates were estimated from CFU/worm measurements over time (**Fig S1B**). At high chloramphenicol concentrations (50-200 µg/mL), change in CFU/worm between 24 and 48 hours after exposure was negative and effectively constant across drug concentrations (**Fig. S1B**), indicating that the antibiotic was effectively suppressing growth of bacteria inside the worms. These data were used to estimate total average death rate of bacteria inside the worms as 0.05-0.1 $hr^{-1}$. If we consider the experimentally derived estimate of death rate (0.05-0.1 $hr^{-1}$) to be accurate, this would imply a very low birth rate of 0.1-0.15 $hr^{-1}$.

*Colonization rate.* Colonization was estimated using a short-time feeding assay. Briefly, *C. elegans* AU37 was fed on live *E. coli* MC4100 at a range of concentrations from ~$10^9$ to $10^6$ CFU/mL (corresponding to colonization rates of 0.1 - 100 CFU/worm/hr). Bacterial density was quantified by dilution plating. At 1 and 4 hours after feeding, 30-60 worms were removed from culture, washed and surface bleached as previously described, and disrupted in a batch; average CFU/worm was determined by dilution plating. The experiment was performed twice, and data were pooled for parameter estimation (**Fig. 2**).

*Feeding rate.* Feeding rate was estimated from the same short-time feeding assay by comparing CFU/mL outside the worms at time 0 and after 10 hours of feeding. Depending on initial concentration, 5-60% of total bacteria in each well were consumed over this time. The resulting ΔCFU/mL was divided by the total number of worms in each well to get an estimated average CFU eaten/worm/hr (**Fig. 2**).

*Robustness to parameter choice.* The transition from bimodal to unimodal population distribution with increasing colonization rate is robust to the parameter values used in simulation (**Fig. S6**). Holding (*b*-*d*) constant, we can observe that this transition occurs around $c/b=1$ across a range of parameter values (compare [*d*=2.44, *b*=2.5] with the other parameter sets). The observed transition is therefore robust to the uncertainty in the parameter values extracted from experimental data (compare [*d*=0.1, *b*=0.16] and [*d*=0.54, *b*=0.6]). However, the variation in total number of bacteria across individual simulated worms increases dramatically as the values of (*b,d*) increase, as does the frequency of extinctions; this is expected behavior for a model where death is stochastic.


15

bioRxiv preprint doi: https://doi.org/10.1101/067173; this version posted August 1, 2016. The copyright holder for this preprint (which was not certified by peer review) is the author/funder, who has granted bioRxiv a license to display the preprint in perpetuity. It is made available under aCC-BY-NC-ND 4.0 International license.

**Microscopy**

After surface bleaching and rinsing as previously described, worms were paralyzed in M9 worm buffer with 10% sodium azide for 10 minutes before transferring to slides with 2% agarose pads for microscopy. Microscopy was performed on a Nikon Eclipse T*i* inverted light microscope system with Chroma filter sets ET-dsRed (49005), ET-YFP (49003), and ET-CFP (49001) and a Pixis 1024 CCD camera; MetaMorph microscopy automation and image analysis software (Molecular Devices) was used for machine control and image capture and integration.

**Stochastic modeling**

Gillespie stochastic simulation of the logistic equation-based stochastic model was performed using the PySCeS environment (Python Simulator for Cellular Systems, http://pysces.sourceforge.net) and StochPy (Stochastic modeling in Python, http://stochpy.sourceforge.net) in iPython Notebook. The tau-leaping method was used in these simulations to reduce computation time. The model used in these simulations (neutralLV.psc) is presented:

*neutralLV.psc*

Modelname: neutralLV

Description: Neutral L-V dynamics with migration

#Note that species 1 and 2 are identical

R1:

$pool > DSRed

(b*DSRed+c)*(1-(DSRed+YFP)/K)

R2:

bioRxiv preprint doi: https://doi.org/10.1101/067173; this version posted August 1, 2016. The copyright holder for this preprint (which was not certified by peer review) is the author/funder, who has granted bioRxiv a license to display the preprint in perpetuity. It is made available under aCC-BY-NC-ND 4.0 International license.

```
$pool > YFP

(b*YFP+c)*(1-(DSRed+YFP)/K)

R3:

DSRed > $pool

d*DSRed

R4:

YFP > $pool

d*YFP

# InitPar

b = 0.6

c = 100

d = 0.54

K = 100000

# InitVar

DSRed = 0

YFP = 0
```

**Acknowledgements**

The laboratory acknowledges support from an NIH R00 Pathways to Independence Award (no. GM085279-02, http://www.nih.gov/), an R01 (no. GM102311-01, http://www.nih.gov/), National Science Foundation CAREER Award (no. PHY-1055154, http://www.nsf.gov/), Pew Fellowship (no. 2010-000224-007,

bioRxiv preprint doi: https://doi.org/10.1101/067173; this version posted August 1, 2016. The copyright holder for this preprint (which was not certified by peer review) is the author/funder, who has granted bioRxiv a license to display the preprint in perpetuity. It is made available under aCC-BY-NC-ND 4.0 International license.

http://www.pewtrusts.org/), Sloan Foundation Fellowship (no. BR2011-066, http://www.sloan.org/sloan-research-fellowships/), and an NIH New Innovator Award (no. DP2, http://commonfund.nih.gov/newinnovator/). The funders had no role in study design, data collection and analysis, decision to publish, or preparation of the manuscript.

**Competing Interests**

The authors have no competing interests to declare.

**References**

1. Palmer C, Bik EM, DiGiulio DB, Relman DA, Brown PO. Development of the Human Infant Intestinal Microbiota. PLoS Biol. 2007 Jun 26;5(7):e177.

2. Wu GD, Chen J, Hoffmann C, Bittinger K, Chen Y-Y, Keilbaugh SA, et al. Linking Long-Term Dietary Patterns with Gut Microbial Enterotypes. Science. 2011 Oct 7;334(6052):105–8.

3. Tilman D. Niche tradeoffs, neutrality, and community structure: A stochastic theory of resource competition, invasion, and community assembly. Proc Natl Acad Sci U S A. 2004 Jul 27;101(30):10854–61.

4. Loudon AH, Venkataraman A, Van Treuren W, Woodhams DC, Parfrey LW, McKenzie VJ, et al. Vertebrate Hosts as Islands: Dynamics of Selection, Immigration, Loss, Persistence, and Potential Function of Bacteria on Salamander Skin. Front Microbiol [Internet]. 2016 Mar 16 [cited 2016 Jun 21];7. Available from: http://www.ncbi.nlm.nih.gov/pmc/articles/PMC4793798/

5. Van den Abbeele P, Grootaert C, Marzorati M, Possemiers S, Verstraete W, Gerard P, et al. Microbial Community Development in a Dynamic Gut Model Is Reproducible, Colon Region Specific, and Selective for Bacteroidetes and Clostridium Cluster IX. Appl Environ Microbiol. 2010 Aug;76(15):5237–46.

6. Faith JJ, Guruge JL, Charbonneau M, Subramanian S, Seedorf H, Goodman AL, et al. The Long-Term

bioRxiv preprint doi: https://doi.org/10.1101/067173; this version posted August 1, 2016. The copyright holder for this preprint (which was not certified by peer review) is the author/funder, who has granted bioRxiv a license to display the preprint in perpetuity. It is made available under aCC-BY-NC-ND 4.0 International license.

Stability of the Human Gut Microbiota. Science [Internet]. 2013 Jul 5 [cited 2013 Aug 9];341(6141). Available from: http://www.sciencemag.org/content/341/6141/1237439

7. Goodman AL, Kallstrom G, Faith JJ, Reyes A, Moore A, Dantas G, et al. Extensive personal human gut microbiota culture collections characterized and manipulated in gnotobiotic mice. Proc Natl Acad Sci. 2011 Apr 12;108(15):6252–7.

8. Costello EK, Stagaman K, Dethlefsen L, Bohannan BJM, Relman DA. The Application of Ecological Theory Toward an Understanding of the Human Microbiome. Science. 2012 Jun 8;336(6086):1255–62.

9. Venkataraman A, Bassis CM, Beck JM, Young VB, Curtis JL, Huffnagle GB, et al. Application of a neutral community model to assess structuring of the human lung microbiome. mBio. 2015;6(1).

10. Macfarlane GT, Macfarlane LE. Acquisition, Evolution and Maintenance of the Normal Gut Microbiota. Dig Dis. 2009;27:90–8.

11. Roeselers G, Mittge EK, Stephens WZ, Parichy DM, Cavanaugh CM, Guillemin K, et al. Evidence for a core gut microbiota in the zebrafish. ISME J. 2011;5(10):1595–608.

12. Rawls JF, Mahowald MA, Ley RE, Gordon JI. Reciprocal Gut Microbiota Transplants from Zebrafish and Mice to Germ-free Recipients Reveal Host Habitat Selection. Cell. 2006;127(2):423–33.

13. Dominguez-Bello MG, Blaser MJ, Ley RE, Knight R. Development of the Human Gastrointestinal Microbiota and Insights From High-Throughput Sequencing. Gastroenterology. 2011 May;140(6):1713–9.

14. Dethlefsen L, Eckburg PB, Bik EM, Relman DA. Assembly of the human intestinal microbiota. Trends Ecol Evol. 2006 Sep;21(9):517–23.

15. McCafferty J, Mühlbauer M, Gharaibeh RZ, Arthur JC, Perez-Chanona E, Sha W, et al. Stochastic changes over time and not founder effects drive cage effects in microbial community assembly in a mouse model.

bioRxiv preprint doi: https://doi.org/10.1101/067173; this version posted August 1, 2016. The copyright holder for this preprint (which was not certified by peer review) is the author/funder, who has granted bioRxiv a license to display the preprint in perpetuity. It is made available under aCC-BY-NC-ND 4.0 International license.

ISME J. 2013 Nov;7(11):2116–25.

16. Yilmaz LS, Walhout AJM. Worms, bacteria, and micronutrients: an elegant model of our diet. Trends Genet [Internet]. [cited 2014 Sep 22]; Available from: http://www.sciencedirect.com/science/article/pii/S0168952514001231

17. Portal-Celhay C, Bradley ER, Blaser MJ. Control of intestinal bacterial proliferation in regulation of lifespan in Caenorhabditis elegans. BMC Microbiol. 2012;12:49.

18. Gillespie DT. Exact stochastic simulation of coupled chemical reactions. J Phys Chem. 1977 Dec 1;81(25):2340–61.

19. Goel N, Richter-Dyn N. Stochastic Models in Biology. Academic Press Inc; 1974. 265 p.

20. Jemielita M, Taormina MJ, Burns AR, Hampton JS, Rolig AS, Guillemin K, et al. Spatial and Temporal Features of the Growth of a Bacterial Species Colonizing the Zebrafish Gut. mBio. 2014 Dec 31;5(6):e01751-14.

21. Kot M. Elements of Mathematical Ecology. Cambridge University Press; 2001.

22. Gerstbrein B, Stamatas G, Kollias N, Driscoll M. In vivo spectrofluorimetry reveals endogenous biomarkers that report healthspan and dietary restriction in Caenorhabditis elegans. Aging Cell. 2005 Jun 1;4(3):127–37.

23. Wu D, Rea SL, Yashin AI, Johnson TE. Visualizing hidden heterogeneity in isogenic populations of C. elegans. Exp Gerontol. 2006 Mar;41(3):261–70.

24. Chow DK, Glenn CF, Johnston JL, Goldberg IG, Wolkow CA. Sarcopenia in the Caenorhabditis elegans pharynx correlates with muscle contraction rate over lifespan. Exp Gerontol. 2006 Mar;41(3):252–60.

25. Garigan D, Hsu A-L, Fraser AG, Kamath RS, Ahringer J, Kenyon C. Genetic Analysis of Tissue Aging in

bioRxiv preprint doi: https://doi.org/10.1101/067173; this version posted August 1, 2016. The copyright holder for this preprint (which was not certified by peer review) is the author/funder, who has granted bioRxiv a license to display the preprint in perpetuity. It is made available under aCC-BY-NC-ND 4.0 International license.

Caenorhabditis elegans: A Role for Heat-Shock Factor and Bacterial Proliferation. Genetics. 2002 Jul 1;161(3):1101–12.

26. Wiles TJ, Jemielita ML, Baker RP, Schlomann BH, Logan SL, Ganz J, et al. Host Gut Motility and Bacterial Competition Drive Instability in a Model Intestinal Microbiota. bioRxiv. 2016 May 12;52985.

27. Ii RCP, Penley MJ, Morran LT. The Integral Role of Genetic Variation in the Evolution of Outcrossing in the Caenorhabditis elegans-Serratia marcescens Host-Parasite System. PLOS ONE. 2016 Apr 27;11(4):e0154463.

28. Hubbell SP. The Unified Neutral Theory of Biodiversity and Biogeography (MPB-32). Princeton University Press; 2001. 394 p.

29. Portal-Celhay C, Blaser MJ. Competition and Resilience between Founder and Introduced Bacteria in the Caenorhabditis elegans Gut. Infect Immun. 2012 Mar 1;80(3):1288–99.

30. Aballay A, Yorgey P, Ausubel FM. Salmonella typhimurium proliferates and establishes a persistent infection in the intestine of Caenorhabditis elegans. Curr Biol. 2000;10(23):1539–42.

31. Samuel BS, Rowedder H, Braendle C, Félix M-A, Ruvkun G. Caenorhabditis elegans responses to bacteria from its natural habitats. Proc Natl Acad Sci. 2016 Jun 17;201607183.

32. Berg M, Stenuit B, Ho J, Wang A, Parke C, Knight M, et al. Assembly of the Caenorhabditis elegans gut microbiota from diverse soil microbial environments. ISME J [Internet]. 2016 Jan 22 [cited 2016 Feb 1]; Available from: http://www.nature.com/ismej/journal/vaop/ncurrent/full/ismej2015253a.html

33. Grant AJ, Restif O, McKinley TJ, Sheppard M, Maskell DJ, Mastroeni P. Modelling within-Host Spatiotemporal Dynamics of Invasive Bacterial Disease. PLOS Biol. 2008 Apr 8;6(4):e74.

34. Lieberman TD, Michel J-B, Aingaran M, Potter-Bynoe G, Roux D, Jr MRD, et al. Parallel bacterial

bioRxiv preprint doi: https://doi.org/10.1101/067173; this version posted August 1, 2016. The copyright holder for this preprint (which was not certified by peer review) is the author/funder, who has granted bioRxiv a license to display the preprint in perpetuity. It is made available under aCC-BY-NC-ND 4.0 International license.

evolution within multiple patients identifies candidate pathogenicity genes. Nat Genet. 2011 Dec;43(12):1275–80.

35. Coward C, Diemen PM van, Conlan AJK, Gog JR, Stevens MP, Jones MA, et al. Competing Isogenic Campylobacter Strains Exhibit Variable Population Structures In Vivo. Appl Environ Microbiol. 2008 Jun 15;74(12):3857–67.

36. Abel S, Wiesch PA zur, Davis BM, Waldor MK. Analysis of Bottlenecks in Experimental Models of Infection. PLOS Pathog. 2015 Jun 11;11(6):e1004823.

37. Stiernagle T. Maintenance of C. elegans. Community TC elegans R, editor. WormBook [Internet]. 2006 Feb 11; Available from: http://www.wormbook.org

38. Moy TI, Conery AL, Larkins-Ford J, Wu G, Mazitschek R, Casadei G, et al. High-Throughput Screen for Novel Antimicrobials using a Whole Animal Infection Model. Acs Chem Biol. 2009 Jul 17;4(7):527–33.

39. Choi K-H, Schweizer HP. mini-Tn7 insertion in bacteria with single attTn7 sites: example Pseudomonas aeruginosa. Nat Protoc. 2006;1(1):153–61.

40. Pfister R, Schwarz KA, Janczyk M, Dale R, Freeman JB. Good things peak in pairs: a note on the bimodality coefficient. Front Psychol [Internet]. 2013 Oct 2 [cited 2016 May 10];4. Available from: http://www.ncbi.nlm.nih.gov/pmc/articles/PMC3791391/

bioRxiv preprint doi: https://doi.org/10.1101/067173; this version posted August 1, 2016. The copyright holder for this preprint (which was not certified by peer review) is the author/funder, who has granted bioRxiv a license to display the preprint in perpetuity. It is made available under aCC-BY-NC-ND 4.0 International license.

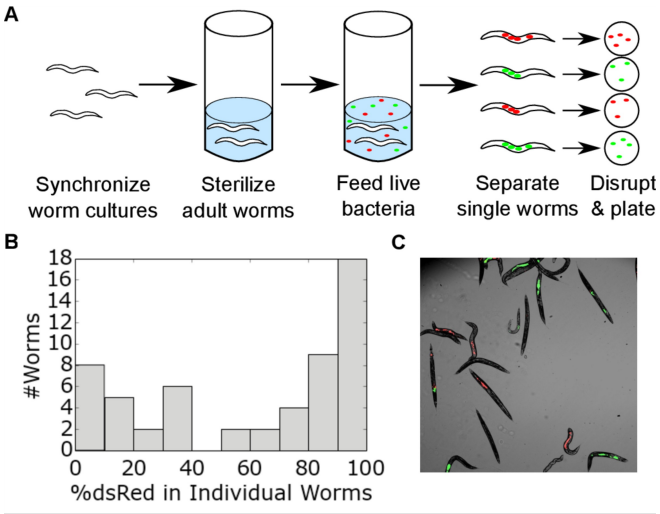


**Fig. 1. Stochastic colonization produces bimodal community composition in the *C. elegans* intestine.** (A) Illustration of experimental procedure. Briefly, synchronized adult worms with germ-free intestines were fed for eight days on a 50/50 mixture of live *E. coli* ($10^6$ CFU/mL in liquid culture) labeled with dsRed or YFP, then individual worms were isolated and disrupted to obtain intestinal contents. (B) After eight days of colonization, we observed a bimodal distribution in bacterial community composition (pooled data from three independent experiments, n=56). (c) Bimodal community composition can be seen in fluorescence microscopy (three-channel overlaid image).

bioRxiv preprint doi: https://doi.org/10.1101/067173; this version posted August 1, 2016. The copyright holder for this preprint (which was not certified by peer review) is the author/funder, who has granted bioRxiv a license to display the preprint in perpetuity. It is made available under aCC-BY-NC-ND 4.0 International license.

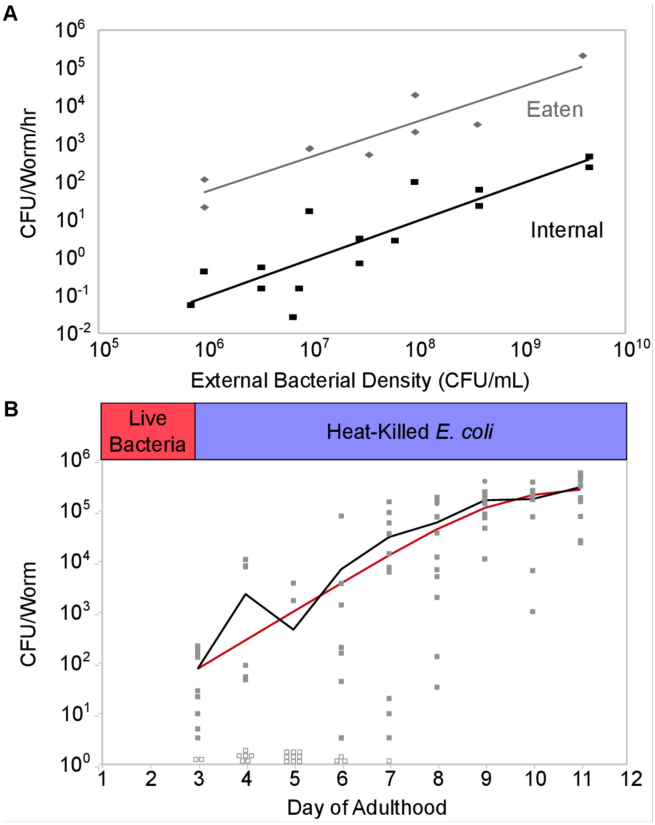


**Fig. 2. Rare migrants grow and colonize the *C. elegans* intestine.** (A) External bacterial density during feeding controls feeding rate (CFU eaten/worm/hr, grey points and line), which in turn reflects the colonization rate (number of internal CFU acquired/worm/hr, black points and line). (B) In the absence of new colonization (see Methods), growth of *E. coli* in the *C. elegans* intestine is described by a logistic model (black line, average CFU/worm; red line, fit of the logistic equation with $r \approx 1.5$ hr$^{-1}$ and $K \approx 2 \times 10^5$ CFU/worm).

bioRxiv preprint doi: https://doi.org/10.1101/067173; this version posted August 1, 2016. The copyright holder for this preprint (which was not certified by peer review) is the author/funder, who has granted bioRxiv a license to display the preprint in perpetuity. It is made available under aCC-BY-NC-ND 4.0 International license.

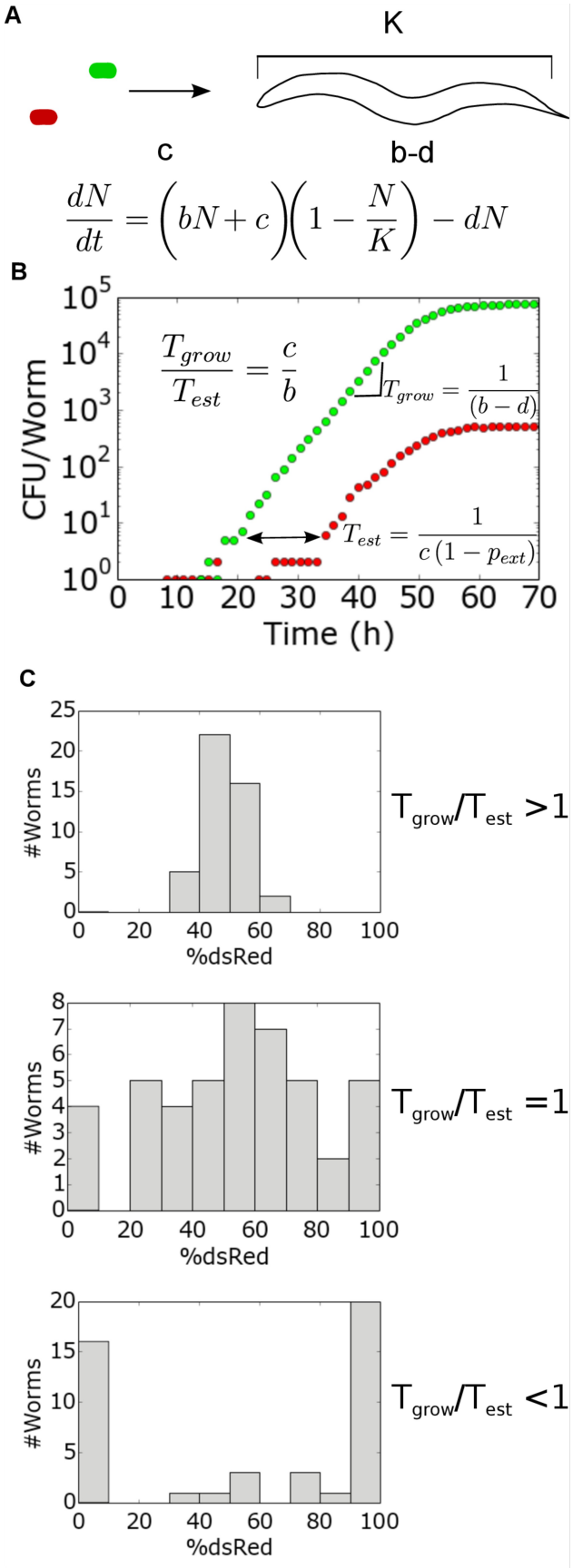

bioRxiv preprint doi: https://doi.org/10.1101/067173; this version posted August 1, 2016. The copyright holder for this preprint (which was not certified by peer review) is the author/funder, who has granted bioRxiv a license to display the preprint in perpetuity. It is made available under aCC-BY-NC-ND 4.0 International license.

**Fig. 3. A stochastic model describes colonization of the *C. elegans* intestine.** (A) Bacterial population dynamics in the worm were modeled using a density-dependent logistic framework. (B) A single Gillespie stochastic simulation (GSSA) run using a low colonization rate ($c$=0.1 $hr^{-1}$) is presented to illustrate the different timescales that determine community assembly in this system. In simulations, worms were colonized with a 50/50 mix of identical bacterial strains, shown here as green and red points. $T_{grow}$ is the characteristic timescale of colony growth inside the worm, and $T_{est}$ is the expected time between successful colonization events. (C) Simulations were performed at a range of colonization rates to illustrate how the critical ratio $T_{grow}/T_{est}$ = c/$b$ controls the transition from bimodal to unimodal community composition.

bioRxiv preprint doi: https://doi.org/10.1101/067173; this version posted August 1, 2016. The copyright holder for this preprint (which was not certified by peer review) is the author/funder, who has granted bioRxiv a license to display the preprint in perpetuity. It is made available under aCC-BY-NC-ND 4.0 International license.

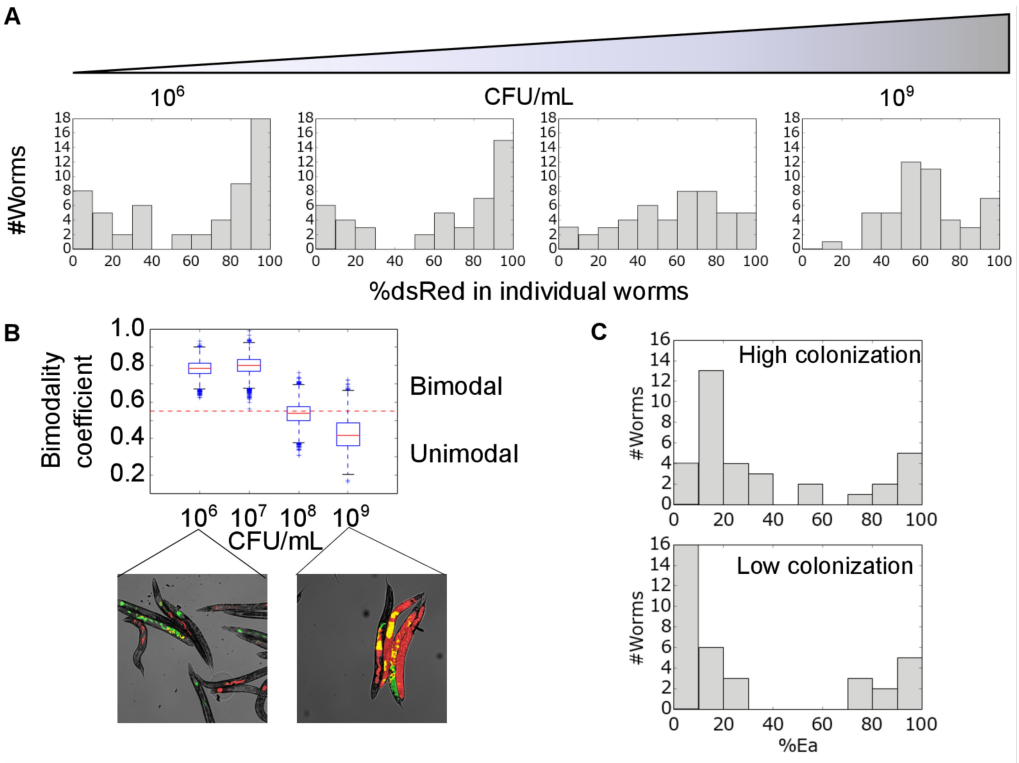


**Fig. 4. Colonization rate tunes heterogeneity of microbial community composition between hosts.** (A) Worms fed on a 50/50 mixture of dsRed and YFP-labeled *E. coli* over a range of concentrations from $10^6$-$10^9$ CFU/mL show a transition from bimodal to unimodal community composition. Data are pooled from 2-3 independent experiments (n=48-56 worms). (B) The transition to bimodality in (A) is confirmed by calculation of the bimodality coefficient (see Methods) for these data (bootstrap confidence intervals over 10,000 runs, red dashed line indicates $BC_{crit}$=0.55) and by direct observation of intestinal communities via fluorescence microscopy. (C) The transition to bimodality was observed when worms were fed on a 50/50 mixture of *Serratia marcescens* and *Enterobacter aerogenes* under high colonization ($10^8$ CFU/mL) and low colonization ($10^6$ CFU/mL) conditions for five days.

bioRxiv preprint doi: https://doi.org/10.1101/067173; this version posted August 1, 2016. The copyright holder for this preprint (which was not certified by peer review) is the author/funder, who has granted bioRxiv a license to display the preprint in perpetuity. It is made available under aCC-BY-NC-ND 4.0 International license.

**Table 1. Parameter estimates used in the stochastic model.**

| Parameter | Value | Units |
|---|---|---|
| K | $2 * 10^5$ | CFU $worm^{-1}$ |
| b | 0.6 | $hr^{-1}$ |
| d | 0.54 | $hr^{-1}$ |
| c | 0.1 – 100 | CFU $worm^{-1}$ $hr^{-1}$ |